sciendo International Journal of Mathematics and Computer in Engineering 3(2) (2025) 185–200

International Journal of Mathematics and Computer in Engineering

https://sciendo.com/journal/IJMCE

Original Study

Considerable traveling wave solutions of the generalized Hietarinta-type equation

Adnan Ahmad Mahmud[1†]

[1] Saro High School for Boys, Sulaymaniyah General Directory of Education, Ministry of Education, Sulaymaniyah, 46001, Iraq

Communicated by Carlo Cattani; Received: 22.01.2024; Accepted: 04.04.2024; Online: 20.09.2024

Abstract

This work utilizes the modified extended tanh − function approach effectively in order to scientifically deduce semi-analytic traveling wave solutions for the (2+1)-dimensional fourth-order non-linear generalized Hietarinta-type problem, leading to previously unidentified satisfactory solutions. The proposed model is transformed into a fourth-order non-linear ordinary differential equation via a traveling wave transformation. Some periodic-solitary, original, and oscillating wave solutions to the model under experimentation are acquired in mixed complex trigonometric and logarithmic functions combined with hyperbolic trigonometric functions, and complex rational functions. Assorted solutions are shown using two- and three-dimensional graphics and suitable arbitrary parameters to demonstrate their physical and dynamic results. Two-dimensional graphs are shown how changes in time formally impact the features and structures of the solution. The free parameters (unrestricted parameters) that keep going in the solutions have a big impact on the dynamic behavior of the solutions. Traveling wave, oscillating, periodic, and breather wave solutions are also figured out with the help of the computational operation that gives values to the free parameters.

Keywords: Modified extended tanh method, generalized Hietarinta-type equation, traveling wave transformation, graphs.
AMS 2020 codes: 35Dxx; 35C07; 65Mxx; 45Kxx.

1 Introduction

It must be remembered that exact solutions to non-linear partial differential equations (PDEs) play a critical role in drawing attention to a wide range of peculiar and intricate characteristics that arise in a variety of applied scientific domains. Symbolic algorithmic programs such as Maple, MATLAB, and Mathematica significantly facilitate the process for mathematicians, physicists, and engineers to explore a wide range of new solutions for non-linear PDEs. These programs offer various analytic and numerical methods, making the framework more accessible and streamlined. Analytic and semi-analytic techniques for resolving linear and nonlinear operational models have been strengthened through diverse methodologies throughout previous works. The fundamental basis for introducing the material is the extended literature on addressing mathematical queries using semi-analytic or analytic methods. Investigators from all around the world are trying to apply these procedures, just as mathematical models with applications in chemistry, biology, physics, and engineering, have recently been solved using these methods. Another argument is that readers may feel certain that these techniques produce appropriate, correct affirmations of the models by complementing the model with computations. Numerous modified and extended versions of the semi-analytic methods have been applied for the illustration of the modified version

†Corresponding author.
Email address: mathematic79@yahoo.com

sciendo ISSN 2956-7068 doi:10.2478/ijmce-2025-0015 sciendo

of $\tanh-$ function and the extended rational sinh-cosh function methods [1], the modified performance method of the exponential functions [2], Bernoulli and its improved version methods [3, 4], the Laplace transformation method has been applied to the features of the Caputo-fractional derivatives [5], the improved version of Bernoulli combined with the methods related to the hyperbolic trigonometric functions [6–8], the new extended direct algebraic method employed [9], the sine-Gordon expansion method and its rational version have been applied [10], the development version of the ultra-spherical wavelet method utilized [11], a Lie symmetry analysis employed [12], the Hirota's bilinear method is considered [13], describing an auxiliary equation approach [14].

The nonlinear fourth-order (2+1)-dimensional generalized Hietarinta-type equation that we investigated has the following arrangement:

$$\begin{gathered}\alpha_1\left(6u_xu_{xx}+u_{xxxx}\right)+\alpha_2\left(3u_tu_{tt}+u_{xt}v_{tt}+u_{xttt}\right)+\gamma_1u_{yt}+\gamma_2u_{xx}+\gamma_3u_{xt}+\gamma_4u_{xy}+\gamma_5u_{yy}=0\\ v_x=u,\end{gathered}\tag{1}$$

where $\alpha_1,\alpha_2,\gamma_i$ for $i=1,2,\cdots,5$ are parameters to be determined later, and α_2 represents the nonlinear coefficient for a generalized Hietarinta-type equation. The studied model represents the dispersion waveform.

Numerous academicians have conducted investigations into the various interpretations of (1) employing more methodological approaches, which include the bilinear method [15], the Hirota bilinear method and Bell polynomials [16, 17]. If you are seeking a unique form of solution that is logically localized in every possible direction, semi-analytic solutions and their interactions are an amazing place to start [18–21]. The utilized method is trustworthy, dependable, and more practical for solving different mathematical models. To provide evidence of the prior declaration, one can inspect how many researchers applied this method and other different performances, herein are some sources [22–26]. The lump solutions to the studied model by utilizing the symbolic computation method have been presented in [27].

Sub-sequential sentences are specialized for the extraction of how these methods apply to different mathematical models, the generalized Kudryashov, generalized Riccati equation mapping, the unified method, the generalized exponential rational function method, and the modified extended $\tanh-$ expansion method [28–31], two new modifications for the trigonometric and hyperbolic trigonometric function methods [32], in these dissertations, some important applications of semi-analytic methods have been represented [33, 34], and the references contained therein.

The rest of the paper is organized as follows: Literature is reviewed related to the fourth-order non-linear (2+1)-dimensional generalized Hietarinta-type equation in Section 1. After that, in Section 2, the configuration of the mentioned procedure is given, briefly. In Section 3, the suggested approach is applied to the disseminated model, and its acquired solutions are demonstrated graphically. Section 4 focusses on the result and discussion; here we present the physical behaviors of the figures. Moreover, numerical simulations of the outcomes and figures are demonstrated. Finally, in Section 5, finalizing and ending views are reported.

2 Structure of the modified extended $\tanh-$ function method

The studied method is abbreviated into the following five steps:

Step 1. The following nonlinear partial differential equation is considered.

$$\Phi(\Lambda,\Lambda_x,\Lambda_t,\Lambda_y,\Lambda_{xt},\Lambda_{xx},\Lambda_{yt},\Lambda_{xyt},\cdots)=0,\tag{2}$$

where $\Lambda=\Lambda(x,y,t)$. By operating

$$\Lambda(x,y,t)=\mathscr{X}(\mathscr{T}),\ \mathscr{T}=\nu_1x+\nu_2y-\nu_3t.\tag{3}$$

The parameters ν_1, ν_2 and ν_3 are arbitrary and non-zero parameters. They represent the straight-line velocity, magnitude of motion, and thickness of wave propagation speed, respectively. Substituting equation (3) into equation (2) yields the follows

$$\mathcal{N}(\mathcal{Z},\mathcal{Z}',\mathcal{Z}'',\cdots)=0, \tag{4}$$

where

$$\mathcal{Z}=\mathcal{Z}(\mathcal{T}),\ \mathcal{Z}'=\frac{d\mathcal{Z}}{d\mathcal{T}},\ \mathcal{Z}''=\frac{d^2\mathcal{Z}}{d\mathcal{T}^2},\cdots.$$

Step 2. Consider equation (4) for the subsequent potential solution:

$$\mathcal{Z}(\mathcal{T})=a_0+\sum_{i=1}^{m}(a_i\mathcal{H}^i+b_i\mathcal{H}^{-i}). \tag{5}$$

The constants $a_0,a_i,b_i,i=1,\cdots,m$ must be subsequently demonstrated in a way that guarantees either a_m or b_m is not equal to zero, and $\mathcal{H}(\mathcal{T})$ is a function that satisfies the specified Riccati ODE:

$$\mathcal{H}'(\mathcal{T})=b+\mathcal{H}^2(\mathcal{T}), \tag{6}$$

the set-solutions of (6) are established as follows:
Case 1: Suppose that b is negative, then:

$$\mathcal{H}(\mathcal{T})=-\sqrt{-b}\tanh(\sqrt{-b}\mathcal{T}),\text{ or }\mathcal{H}(\mathcal{T})=-\sqrt{-b}\coth(\sqrt{-b}\mathcal{T}). \tag{7}$$

Case 2: Suppose that b is positive, then:

$$\mathcal{H}(\mathcal{T})=\sqrt{b}\tan(\sqrt{b}\mathcal{T}),\ \text{ or }\ \mathcal{H}(\mathcal{T})=-\sqrt{b}\cot(\sqrt{b}\mathcal{T}). \tag{8}$$

Case 3: Suppose that $b=0$, then:

$$\mathcal{H}(\mathcal{T})=-\frac{1}{\mathcal{T}}. \tag{9}$$

Step 3. The value of the positive integer m in equation (4) should be determined using the balance of powers principle, which involves considering the relationship between the highest-order derivatives and the greatest power of the non-linear terms.

Step 4. By substituting equations (5) and (6) into equation (4) and grouping terms with the identical power of $\mathcal{H}^i$ where $i=0,\pm1,\pm2,\cdots$, we acquire a set of algebraic equations. These equations can be solved using software programs to determine the principles of the parameters.

Step 5. A combination of equations (7)-(9) and considering constrained values of parameters may give the exact solution to equation (2).

3 Application

By putting wave transformation (3) to equation (1) and simplifying mathematically, the following result is obtained:

$$\begin{aligned}&\alpha_1\nu_1^4\mathcal{U}^{(4)}+\alpha_2\nu_3^2\nu_1\mathcal{U}^{(3)}+3\alpha_2\nu_3^3\nu_1\mathcal{U}''V''+\beta_2\nu_1^2\mathcal{U}''+\beta_4\nu_2\nu_1\mathcal{U}''+\beta_3\nu_3\nu_1\mathcal{U}''\\&+\beta_5\nu_2^2\mathcal{U}''+\beta_1\nu_2\nu_3\mathcal{U}''+6\alpha_1\nu_1^3\mathcal{U}'\mathcal{U}''+3\alpha_2\nu_3^3\mathcal{U}'\mathcal{U}''=0,\end{aligned} \tag{10}$$

and

$$\nu_1 \mathscr{V}' = \mathscr{U} \to \mathscr{V}'' = \frac{\mathscr{U}'}{\nu_1}, \tag{11}$$

substituting (11) into (10), directly one obtains:

$$\begin{aligned} &\alpha_1 \nu_1^4 \mathscr{U}^{(4)} + \alpha_2 \nu_3^2 \nu_1 \mathscr{U}^{(3)} + \left(\beta_2 \nu_1^2 + \beta_4 \nu_2 \nu_1 + \beta_3 \nu_3 \nu_1 + \beta_5 \nu_2^2 + \beta_1 \nu_2 \nu_3\right) \mathscr{U}'' \\ &+ 6\left(\alpha_1 \nu_1^3 + \alpha_2 \nu_3^3\right) \mathscr{U}' \mathscr{U}'' = 0, \end{aligned} \tag{12}$$

by running integration to (12) one time, we assume $\mathscr{Z}(\cdot)$ at the initial effectiveness is nullified, and then one concludes the outcome with:

$$\begin{aligned} &\alpha_1 \nu_1^4 \mathscr{U}^{(3)} + \alpha_2 \nu_3^2 \nu_1 \mathscr{U}'' + 3\left(\alpha_1 \nu_1^3 + \alpha_2 \nu_3^3\right) \left(\mathscr{U}'\right)^2 \\ &+ \left(\beta_2 \nu_1^2 + \beta_4 \nu_2 \nu_1 + \beta_3 \nu_3 \nu_1 + \beta_5 \nu_2^2 + \beta_1 \nu_2 \nu_3\right) \mathscr{U}' = 0, \end{aligned} \tag{13}$$

by replacing $\mathscr{U}' = \mathscr{Z}$ in (13), the process ends up by:

$$\alpha_1 \nu_1^4 \mathscr{Z}'' + 3\left(\alpha_1 \nu_1^3 + \alpha_2 \nu_3^3\right) \mathscr{Z}^2 + \alpha_2 \nu_3^2 \nu_1 \mathscr{Z}' + \left(\beta_2 \nu_1^2 + \beta_4 \nu_2 \nu_1 + \beta_3 \nu_3 \nu_1 + \beta_5 \nu_2^2 + \beta_1 \nu_2 \nu_3\right) \mathscr{Z} = 0. \tag{14}$$

The resulting ODE that exists in (14) is an authorized equation for functioning the balance principle.

To solve the model in equation (1) using the modified extended tanh− function technique, begin by using the balancing principle in equation (14) to compare $\mathscr{Z}''$ and $\mathscr{Z}^2$. This yields the result $m = 2$, and equation (5) may then be rewritten as:

$$\mathscr{Z} = a_0 + a_1 \mathscr{H} + a_2 \mathscr{H}^2 + \frac{b_1}{\mathscr{H}} + \frac{b_2}{\mathscr{H}^2}, \tag{15}$$

where a_0, a_1, a_2, b_1, b_2 are all parameters to be picked up afterward, whereas $a_2 \neq 0$ or $b_2 \neq 0$, and $\mathscr{H}$ is a function that fulfills the subsequent ODE:

$$\mathscr{H}' = b + \mathscr{H}^2. \tag{16}$$

To get the first and second derivatives, respectively, refer to equation (15). By taking into account equation (16), one may immediately obtain the following:

$$\mathscr{Z}' = 2a_2 b \mathscr{H} + a_1 b + 2a_2 \mathscr{H}^3 + a_1 \mathscr{H}^2 - \frac{2bb_2}{\mathscr{H}^3} - \frac{bb_1}{\mathscr{H}^2} - \frac{2b_2}{\mathscr{H}} - b_1, \tag{17}$$

and

$$\mathscr{Z}'' = 2a_2 b^2 + 8a_2 b \mathscr{H}^2 + 2a_1 b \mathscr{H} + 6a_2 \mathscr{H}^4 + 2a_1 \mathscr{H}^3 + \frac{6b^2 b_2}{\mathscr{H}^4} + \frac{2b^2 b_1}{\mathscr{H}^3} + \frac{8bb_2}{\mathscr{H}^2} + \frac{2bb_1}{\mathscr{H}} + 2b_2. \tag{18}$$

By substituting equations (15)-(18) into equation (13) and simplifying, we gather all the coefficients of $\mathscr{H}^i$, where i ranges from 0 to 8. We then equate the coefficients of the same power of $\mathscr{H}^i$ to zero. Generating a set of algebraic equations for the parameters as follows:

$$\mathscr{C}_i = 0, \text{ where } \mathscr{C}_i \text{ is the coefficient of } \mathscr{H}^i, \text{ for any } i = 0, \mp 1, \mp 2, \mp 3, \mp 4. \tag{19}$$

The system (19) is solved by programs running on computers, and the subsequent illustrations are generated:

Case 1. The following are the parameters that were gathered while solving (19):

$$
\begin{aligned}
&a_0=-\frac{b_2}{b}, a_1=0; a_2=0; b_1=-\frac{2ib_2}{\sqrt{b}}, \alpha_2=-\frac{1000i\alpha_1 b^{3/2}b_2^2\nu_1^3}{(2b^2\nu_1+b_2)^2}, \nu_3=-\frac{i\left(2b^2\nu_1+b_2\right)}{10\sqrt{b}b_2},\\
&\gamma_1=\frac{-2b^2\gamma_4\nu_1^2+ib_2\left(10\sqrt{b}\left(24\alpha_1 b\nu_1^4+\gamma_2\nu_1^2+\gamma_5\nu_2^2\right)+\gamma_4\nu_1\left(10\sqrt{b}\nu_2+i\right)\right)}{\nu_2\left(2b^2\nu_1+b_2\right)}.
\end{aligned}
\tag{20}
$$

The computed parameters in (20) and for the varied characteristics of b the subsequent sub-cases of the outcomes are picked up.

Case 1.1. After solving the Riccati ODE (16) for $b<0$ by performing $\mathscr{H}=-\sqrt{-b}\tanh\left(\sqrt{-b}\mathscr{T}\right)$, the solutions of (1) are identified as.

$$
u_{11}=\frac{b_2\left(b\coth\left(\sqrt{-b}\mathscr{T}\right)-2i\sqrt{-b^2}\left(\log\left(\tanh\left(\sqrt{-b}\mathscr{T}\right)\right)-\log\left(b-i\sqrt{-b^2}\tanh\left(\sqrt{-b}\mathscr{T}\right)\right)\right)\right)}{\sqrt{-b}b^2}, \tag{21}
$$

$$
\begin{aligned}
\nu_{11}=&-\frac{\left(2b^2\nu_1+b_2\right)^2\left(-2i\sqrt{-b^2}\left(\sqrt{-b}\operatorname{csch}\left(\sqrt{-b}\mathscr{T}\right)\operatorname{sech}\left(\sqrt{-b}\mathscr{T}\right)+\frac{i\sqrt{-b}\sqrt{-b^2}\operatorname{sech}^2\left(\sqrt{-b}\mathscr{T}\right)}{b-i\sqrt{-b^2}\tanh\left(\sqrt{-b}\mathscr{T}\right)}\right)\right)}{100\sqrt{-b}b^3b_2\nu_1}\\
&+\frac{\sqrt{-b}b\left(2b^2\nu_1+b_2\right)^2\operatorname{csch}^2\left(\sqrt{-b}\mathscr{T}\right)}{100\sqrt{-b}b^3b_2\nu_1},
\end{aligned}
\tag{22}
$$

where

$$
\mathscr{T}=\nu_1 x+\nu_2 y+\frac{i\left(2b^2\nu_1+b_2\right)}{10\sqrt{b}b_2}t.
$$

Case 1.2. If $b>0$, and $\mathscr{H}=\sqrt{b}\tan\left(\sqrt{b}\mathscr{T}\right)$ designated as an outcome of the Riccati ODE (16), the consequent solutions of (1) turn into:

$$
u_{12}=-\frac{b_2\left(\cot\left(\sqrt{b}\mathscr{T}\right)-2i\left(-\log\left(\tan\left(\sqrt{b}\mathscr{T}\right)\right)+\log\left(-\tan\left(\sqrt{b}\mathscr{T}\right)+i\right)\right)\right)}{b^{3/2}}, \tag{23}
$$

and

$$
\nu_{12}=-\frac{(2b^2\nu_1+b_2)^2\left(-\sqrt{b}\csc^2\left(\sqrt{b}\mathscr{T}\right)-2i\left(-\sqrt{b}\csc\left(\sqrt{b}\mathscr{T}\right)\sec\left(\sqrt{b}\mathscr{T}\right)-\frac{\sqrt{b}\sec^2\left(\sqrt{b}\mathscr{T}\right)}{-\tan\left(\sqrt{b}\mathscr{T}\right)+i}\right)\right)}{b^{3/2}\nu_1}, \tag{24}
$$

herein

$$
\mathscr{L}=\nu_1 x+\nu_2 y+\frac{i\left(2b^2\nu_1+b_2\right)}{10\sqrt{b}b_2}t.
$$

The profiles of the solutions in (23) and (24) have been appointed in the following where: $\nu_1=\frac{3}{4}$, $\nu_2=\frac{2}{3}$, $b=\frac{3}{5}$, $b_2=\frac{3}{2}$, $y=\frac{4}{5}$, and $x,t\in[-10,10]$.

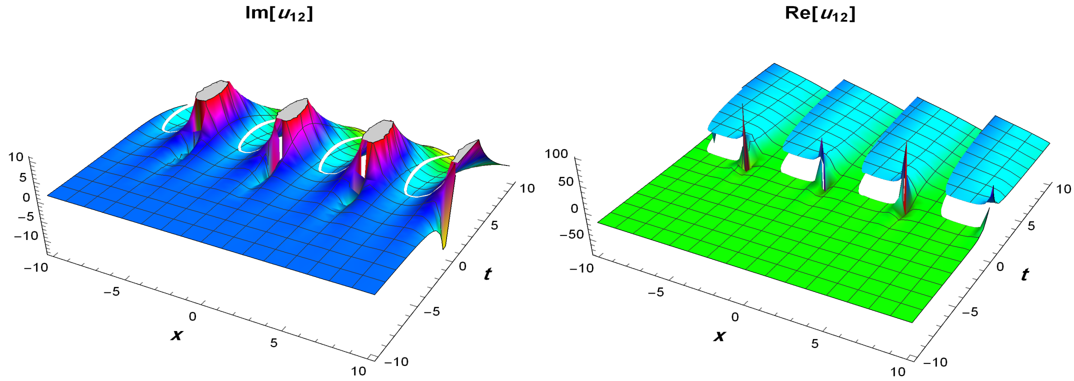

(a) Imaginary part (b) Real part

Fig. 1 Three-dimensional figures of (23).

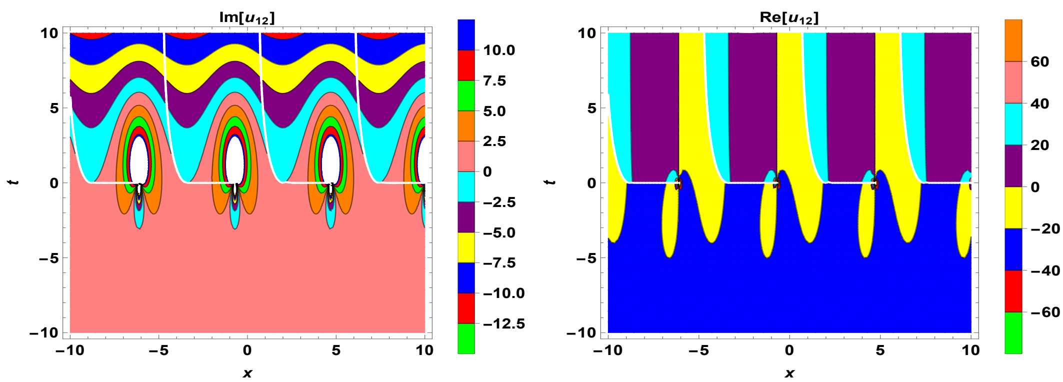

(a) Imaginary part (b) Real part

Fig. 2 Two-dimensional contour surface plots for (23).

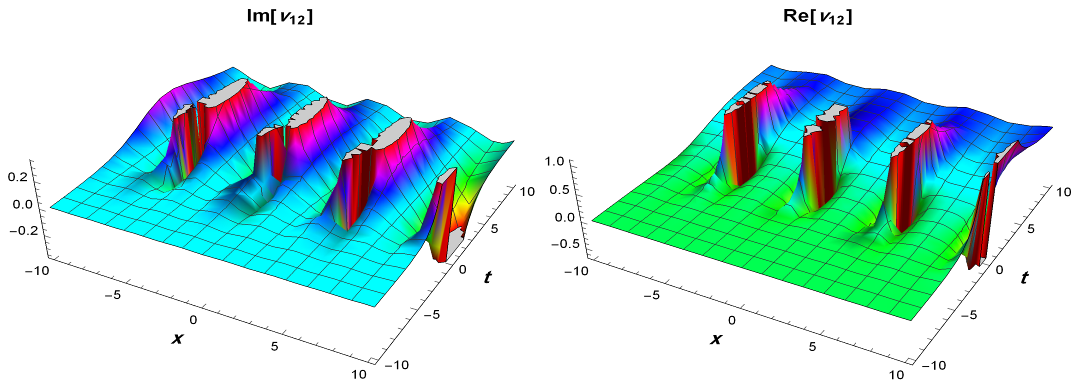

(a) Imaginary part (b) Real part

Fig. 3 Three-dimensional figures of (24).

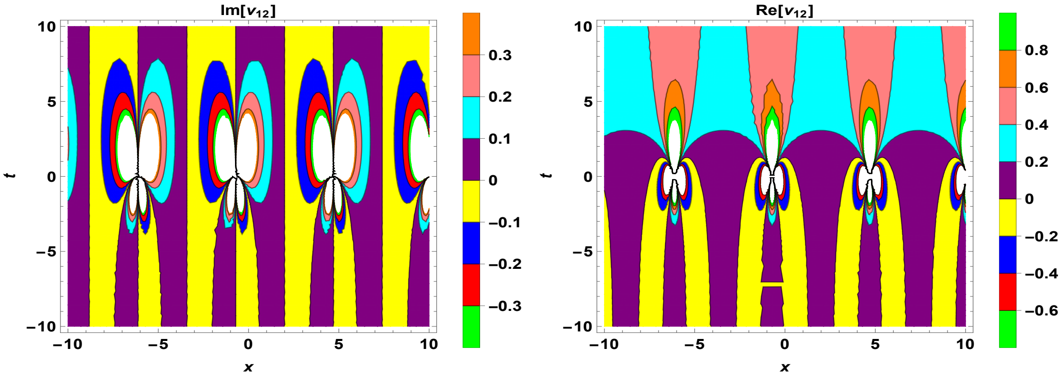

(a) Imaginary part (b) Real part

Fig. 4 Two-dimensional contour surface plots for (24).

In the following three-dimension revolution figures, select $t = \frac{3}{2}, x \in [-10, 10]$.

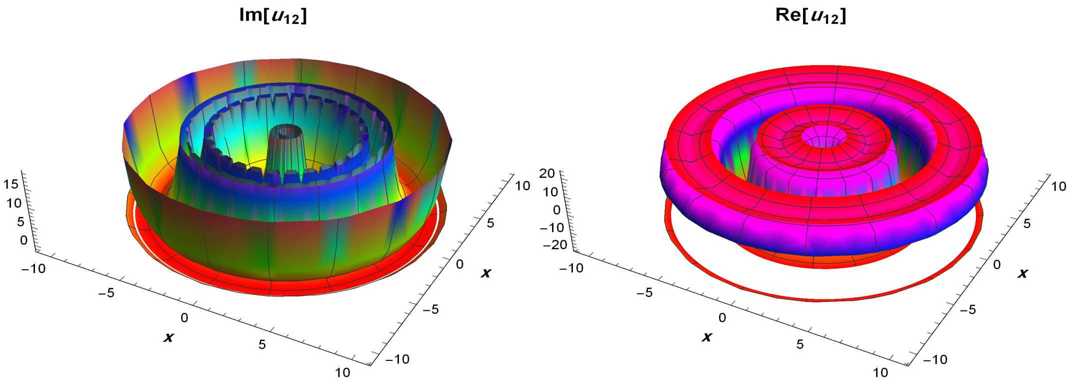

(a) Imaginary part (b) Real part

Fig. 5 3D revolving plots of (23).

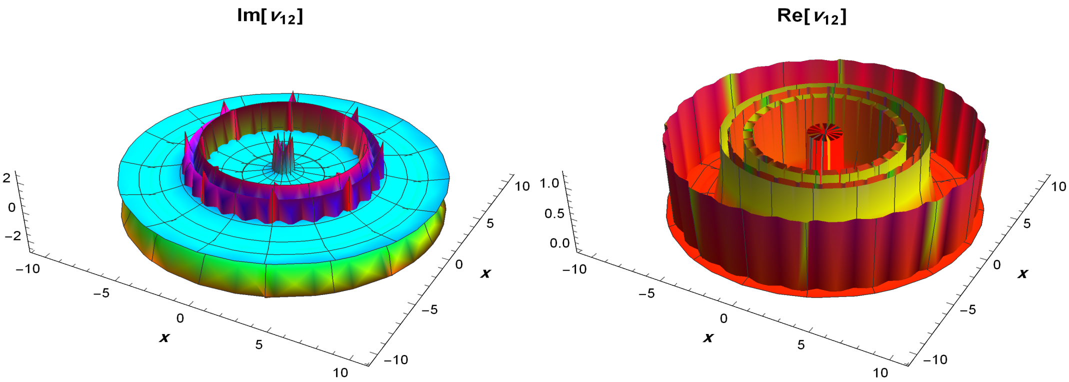

(a) Imaginary part (b) Real part

Fig. 6 3D revolving plots of (24).

Where time-evolution values are given in the legend below and $-20 \leq x \leq 20$ we have the following two dimensional time evolution graphs for (23) and (24):

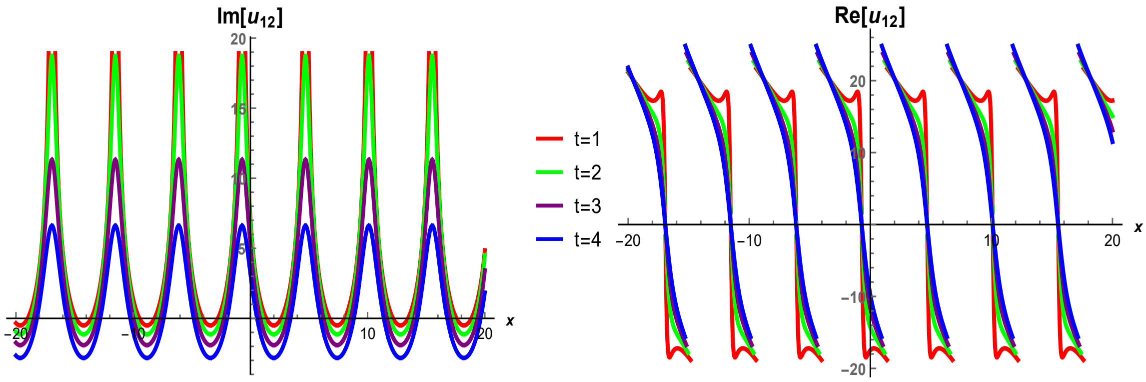

(a) Imaginary part (b) Real part

Fig. 7 2D time-evolution graphs of (23).

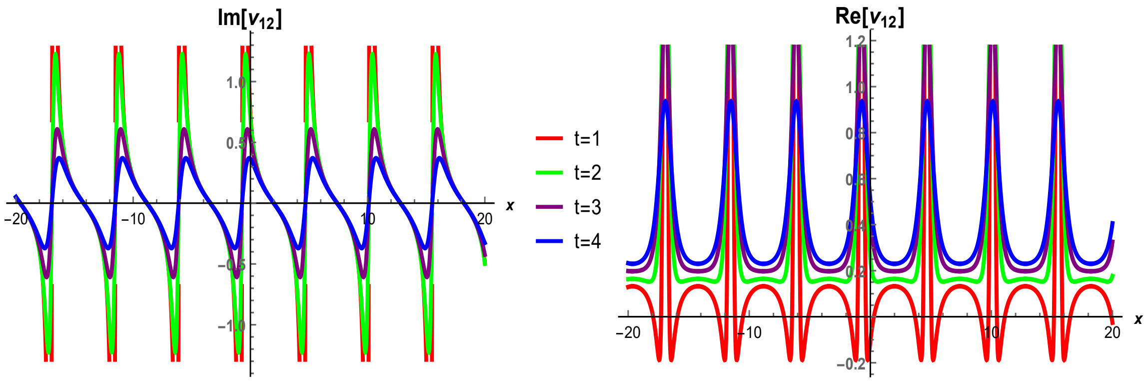

(a) Imaginary part (b) Real part

Fig. 8 2D time-evolution graphs of (24).

Remark 1. A null possibility exists for $b = 0$. One could say that the investigated model has a trivial solution in this particular case.

Remark 2. In this instance, the relevance of choosing parameter values is clear; they define the resulting solutions' characteristics and physical elements.

Case 2. The subsequent parameters are acquired from solving (19):

$$
\begin{aligned}
a_0 &= \frac{6ib\nu_1}{10\sqrt{b}\nu_3 - i}, a_1 = \frac{4\sqrt{b}\nu_1}{10\sqrt{b}\nu_3 - i}, a_2 = \frac{2i\nu_1}{10\sqrt{b}\nu_3 - i}, b_1 = 0, b_2 = 0, \\
\gamma_2 &= \frac{\nu_3\left(5\gamma_1\nu_2 + 12i\alpha_2\sqrt{b}\nu_1\nu_3\right) - 5\gamma_5\nu_2^2 + 5\gamma_4\nu_1\left(\nu_3 - \nu_2\right)}{5\nu_1^2}, \alpha_1 = \frac{i\alpha_2\nu_3^2}{10\sqrt{b}\nu_1^3}.
\end{aligned}
\tag{25}
$$

The obtained parameters in (25) and the sign of the constant b have a central function in generating the following sub-cases of the solutions for the investigated model.

Case 2.1. If $b<0$ and using $\mathscr{H}=-\sqrt{-b}\tanh\left(\sqrt{-b}\mathscr{T}\right)$ as a solution of the Riccati ODE (16), one attains the following solutions to (1):

$$\begin{aligned} u_{21}=&-\frac{2i\nu_1\left(\frac{b\tanh^{-1}\left(\tanh\left(\sqrt{-b}(-\nu_3t+\nu_1x+\nu_2y)\right)\right)}{\sqrt{-b}}-\frac{2i\sqrt{-b^2}\log\left(\cosh\left(\sqrt{-b}(-\nu_3t+\nu_1x+\nu_2y)\right)\right)}{\sqrt{-b}}\right)}{10\sqrt{b}\nu_3-i}\\ &+\frac{2i\nu_1\left(3b\left(-\nu_3t+\nu_1x+\nu_2y\right)+\frac{b\tanh\left(\sqrt{-b}(-\nu_3t+\nu_1x+\nu_2y)\right)}{\sqrt{-b}}\right)}{10\sqrt{b}\nu_3-i}, \end{aligned} \tag{26}$$

and

$$\begin{aligned} v_{21}=&\frac{2i\nu_3^2\left(-\frac{b\text{sech}^2\left(\sqrt{-b}(-\nu_3t+\nu_1x+\nu_2y)\right)}{1-\tanh^2\left(\sqrt{-b}(-\nu_3t+\nu_1x+\nu_2y)\right)}+2i\sqrt{-b^2}\tanh\left(\sqrt{-b}\left(-\nu_3t+\nu_1x+\nu_2y\right)\right)\right)}{10\sqrt{b}\nu_3-i}\\ &+\frac{2i\nu_3^2\left(b\text{sech}^2\left(\sqrt{-b}\left(-\nu_3t+\nu_1x+\nu_2y\right)\right)+3b\right)}{10\sqrt{b}\nu_3-i}. \end{aligned} \tag{27}$$

Case 2.2. The solution of (1) has been retrieved if $b>0$ using $\mathscr{H}=\sqrt{b}\tan\left(\sqrt{b}\mathscr{T}\right)$ as a solution of the Riccati ODE (16).

$$u_{22}=\frac{2i\sqrt{b}\nu_1\left(3\sqrt{b}\mathscr{T}-\tan^{-1}\left(\tan\left(\sqrt{b}\mathscr{T}\right)\right)+\tan\left(\sqrt{b}\mathscr{T}\right)+2i\log\left(\cos\left(\sqrt{b}\mathscr{T}\right)\right)\right)}{10\sqrt{b}\nu_3-i}, \tag{28}$$

and

$$v_{22}=\frac{2i\sqrt{b}\nu_3^2\left(-2i\sqrt{b}\tan\left(\sqrt{b}\mathscr{T}\right)+\sqrt{b}\sec^2\left(\sqrt{b}\mathscr{T}\right)-\frac{\sqrt{b}\sec^2\left(\sqrt{b}\mathscr{T}\right)}{\tan^2\left(\sqrt{b}\mathscr{T}\right)+1}+3\sqrt{b}\right)}{10\sqrt{b}\nu_3-i}, \tag{29}$$

herein $\mathscr{T}=\nu x+\nu_2y-\nu_3t$.

Remark 3. A null possibility occurs for $b=0$. One may claim that the researched model has a trivial solution in this specific circumstance.

Case 3. The succeeding parameters can be determined by resolving the system (19).

$$\begin{aligned} &a_0=3a_2b, a_1=-2ia_2\sqrt{b}, b_1=0, b_2=0, \alpha_2=\frac{1000ia_2^2\alpha_1b^{3/2}\nu_1^3}{(a_2+2\nu_1)^2}, \nu_3=\frac{i(a_2+2\nu_1)}{10a_2\sqrt{b}},\\ &\gamma_2=\frac{a_2\left(10\sqrt{b}\left(24\alpha_1b\nu_1^4-\gamma_5\nu_2^2\right)+\gamma_4\nu_1\left(-10\sqrt{b}\nu_2+i\right)+i\gamma_1\nu_2\right)+2i\nu_1\left(\gamma_4\nu_1+\gamma_1\nu_2\right)}{10a_2\sqrt{b}\nu_1^2}. \end{aligned} \tag{30}$$

Components in (30) are produce the subsequent sub-cases of solutions of (1) by taking into consideration the sign of b.

Case 3.1. If $b<0$ operating $\mathscr{H}=-\sqrt{-b}\tanh\left(\sqrt{-b}\mathscr{T}\right)$ as a solution of the Riccati ordinary differential equation (16), then one obtains the following solutions to (1).

$$u_{31}=a_2\left(\frac{2i\sqrt{-b^2}\log\left(\cosh\left(\sqrt{-b}\mathscr{T}\right)\right)}{\sqrt{-b}}+3b\mathscr{T}-\frac{b\tanh^{-1}\left(\tanh\left(\sqrt{-b}\mathscr{T}\right)\right)}{\sqrt{-b}}+\frac{b\tanh\left(\sqrt{-b}\mathscr{T}\right)}{\sqrt{-b}}\right), \tag{31}$$

and

$$v_{31} = -\frac{(a_2+2\nu_1)^2\left(2i\sqrt{-b^2}\tanh\left(\sqrt{-b}\mathscr{T}\right)+b\operatorname{sech}^2\left(\sqrt{-b}\mathscr{T}\right)-\frac{b\operatorname{sech}^2\left(\sqrt{-b}\mathscr{T}\right)}{1-\tanh^2\left(\sqrt{-b}\mathscr{T}\right)}+3b\right)}{100a_2b\nu_1}, \tag{32}$$

where

$$\mathscr{T} = \nu_1 x + \nu_2 y - \frac{i(a_2+2\nu_1)}{10a_2\sqrt{b}}t.$$

Case 3.2. If $b>0$ operating $\mathscr{H} = \sqrt{b}\tan\left(\sqrt{b}\mathscr{T}\right)$ as a solution of (16), then the obtained solutions of (1) take the formulations below:

$$u_{32} = 3a_2b\mathscr{T} - a_2\sqrt{b}\tan^{-1}\left(\tan\left(\sqrt{b}\mathscr{T}\right)\right) + a_2\sqrt{b}\tan\left(\sqrt{b}\mathscr{T}\right) + 2ia_2\sqrt{b}\log\left(\cos\left(\sqrt{b}\mathscr{T}\right)\right), \tag{33}$$

and

$$v_{32} = \frac{\nu_3^2\left(-2ia_2b\tan\left(\sqrt{b}\mathscr{T}\right)+a_2b\sec^2\left(\sqrt{b}\mathscr{T}\right)-\frac{a_2b\sec^2\left(\sqrt{b}\mathscr{T}\right)}{\tan^2\left(\sqrt{b}\mathscr{T}\right)+1}+3a_2b\right)}{\nu_1}. \tag{34}$$

In (33) and (34) it should be declared that

$$\mathscr{T} = \nu_1 x + \nu_2 y - \frac{i(a_2+2\nu_1)}{10a_2\sqrt{b}}t,$$

when $\nu_1 = \frac{3}{4}, \nu_2 = -\frac{2}{3}, b = \frac{5}{2}, a_2 = -\frac{2}{3}, y = \frac{1}{4}$, and $-10 \le x \le 10$, $-10 \le t \le 10$ the existed solutions in (33) and (34) have the following figures:

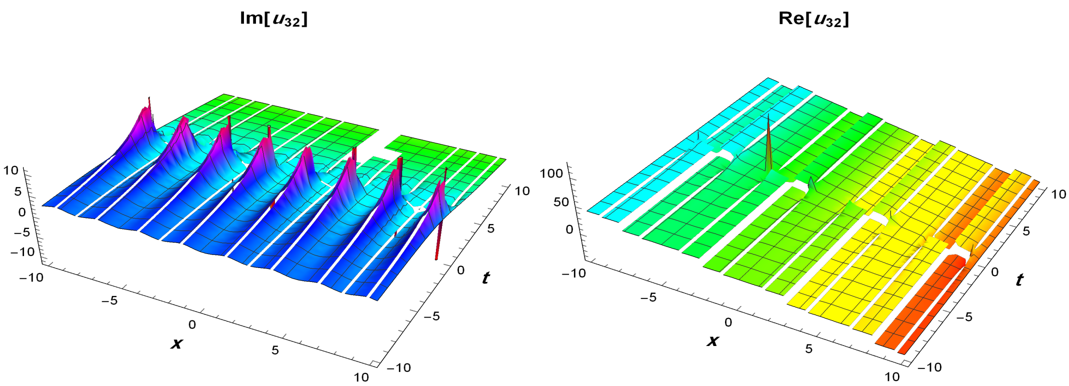

(a) Imaginary part (b) Real part

Fig. 9 Three-dimensional figures of (33).

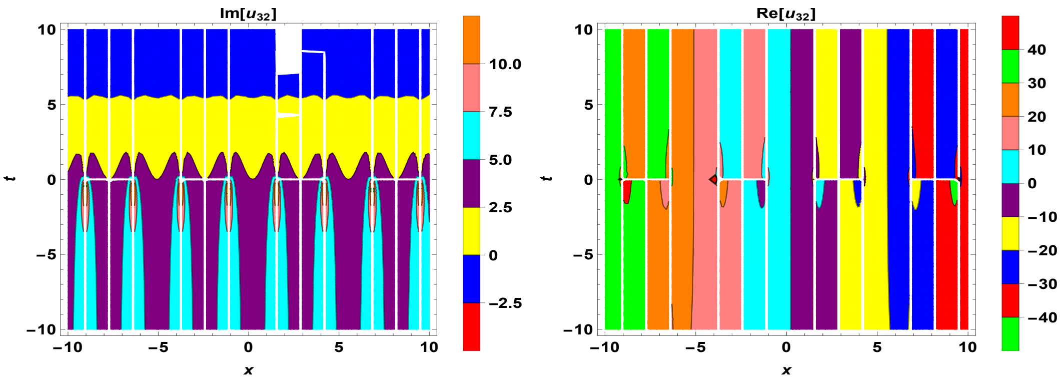

(a) Imaginary part (b) Real part

Fig. 10 Two-dimensional contour surface plots for (33).

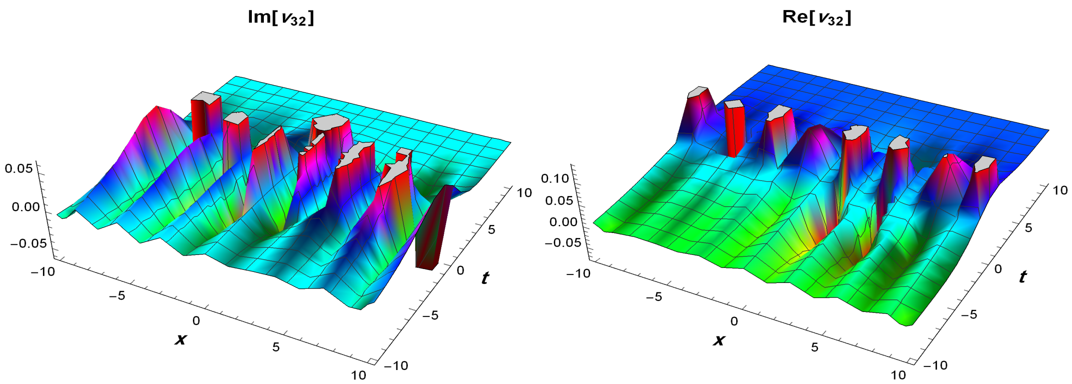

(a) Imaginary part (b) Real part

Fig. 11 Three-dimensional figures of (34).

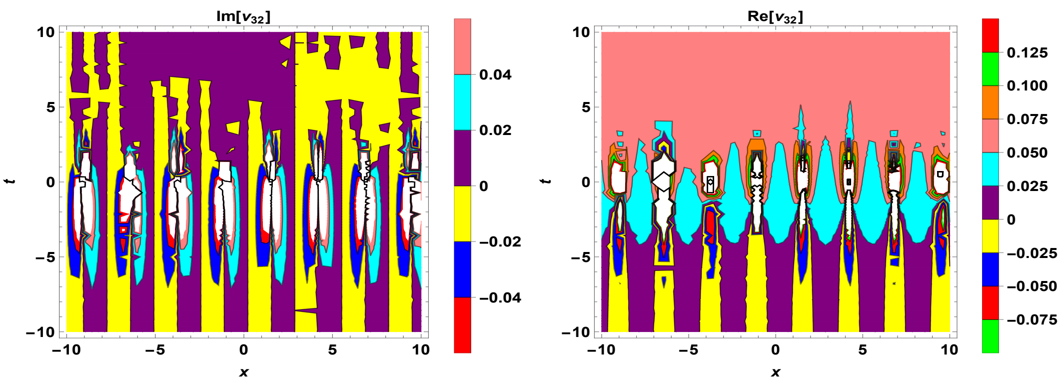

(a) Imaginary part (b) Real part

Fig. 12 Two-dimensional contour surface plots for (34).

Where $t = \frac{2}{3}$, and $-10 \leq x \leq 10$ we have the following three-dimensional revolving figures:

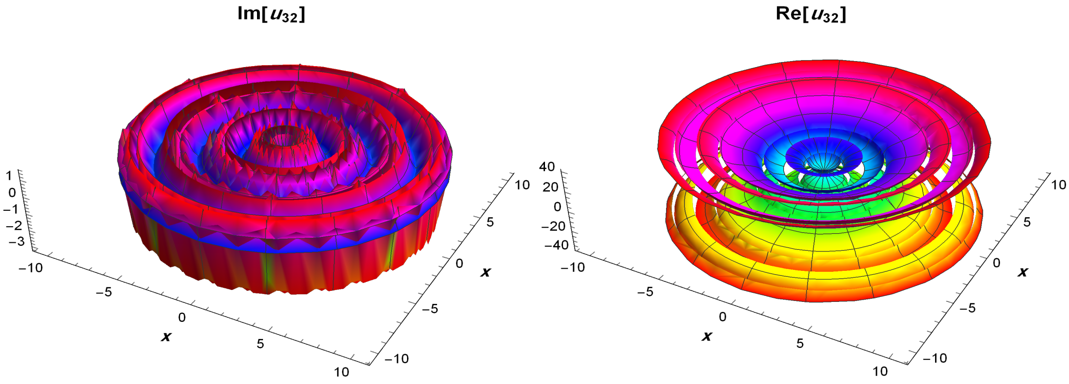

(a) Imaginary part (b) Real part

Fig. 13 3D revolving plot of (33).

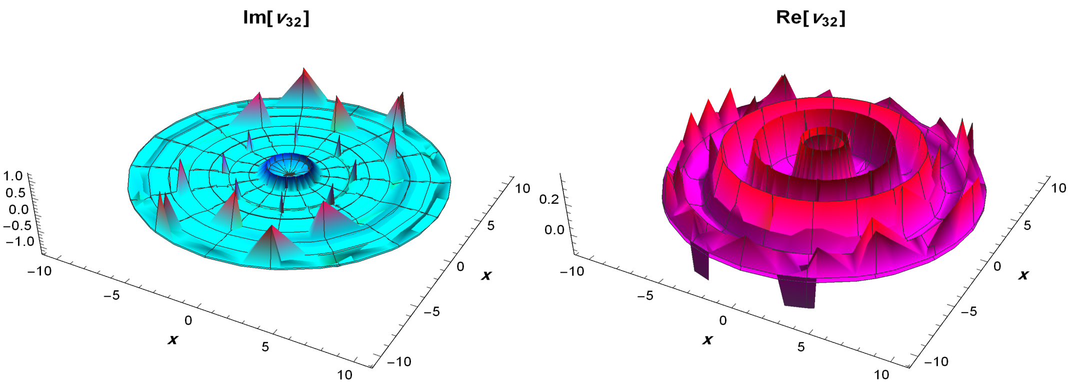

(a) Imaginary part (b) Real part

Fig. 14 3D revolving plot of (34).

When time values are provided in the legend below along with $-10 \leq x \leq 10$ we obtain the following two-dimensional visualizations that illustrate time-evolution impacts on the solution's behaviors.

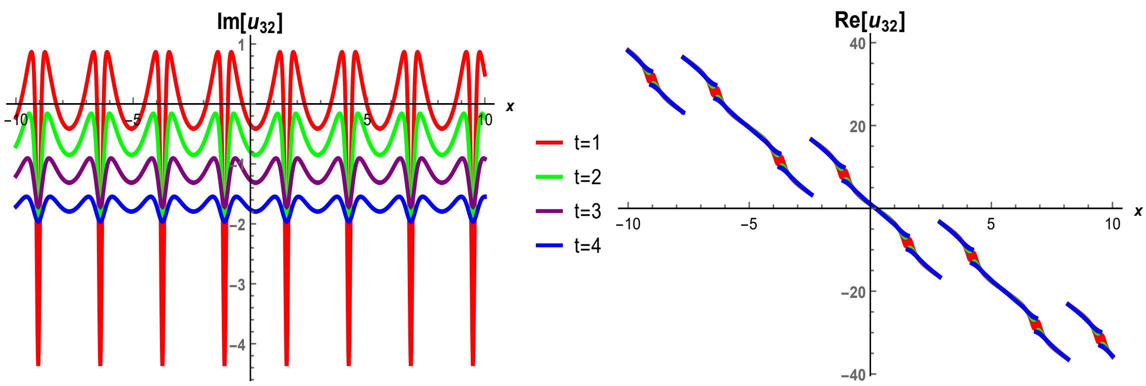

(a) Imaginary part (b) Real part

Fig. 15 2D time-evolution graphs of (33).

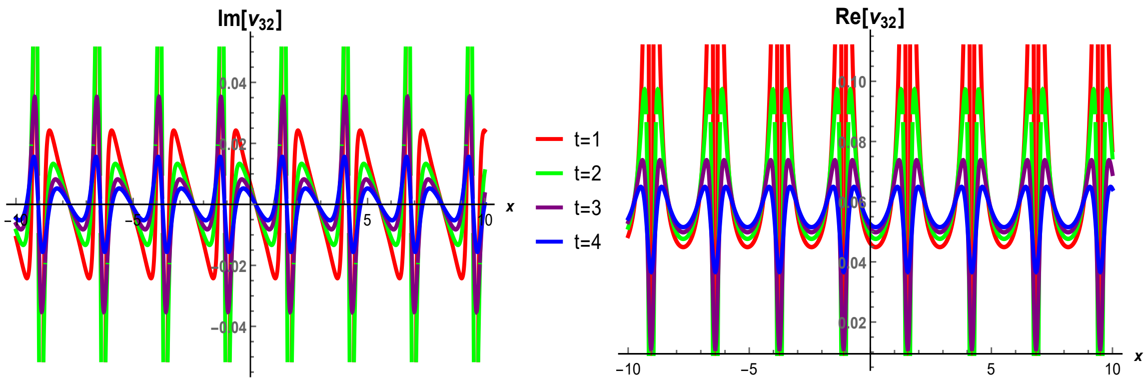

(a) Imaginary part (b) Real part

Fig. 16 2D time-evolution graphs of (34).

Remark 4. A zero-valued value for b cannot be achieved as it leaves part of the coefficients undefined, and hence, in this circumstance, one may say (1) has only a trivial solution.

4 Result and discussion

The newly discovered explicit wave configurations in the generalized Hietarinta-type dynamic wave equation have been addressed. Various types of solutions such as lump-periodic, rouge waves, breather-type, and two-wave solutions have been reconstructed by using the modified extended tanh− function method. Proficient individuals may extend the obtained results to the other fields of physics or mathematics. Through the utilization of algorithms for computation, we have validated our results by reintroducing them into the specified equation. Our study is more familiar compared to the previous investigations. To declare this, some particular recent studies have been mentioned, for instance: In [27], the lump solutions have been found for this model. In [17], several kinds of wave structures have been generated through the application of Hirota's bilinear method and diverse test function viewpoints. The waveform and the figures are mostly affected by choosing appropriate numerical values for free parameters that remain in the solutions. For equations (23) and (24), the free parameters have been selected by: $v_1 = \frac{3}{4}$, $v_2 = \frac{2}{3}$, $b = \frac{3}{5}$, $b_2 = \frac{3}{2}$, $y = \frac{4}{5}$. While the intervals also have a great impact on the appearance of the solutions, here we choose $-10 \leq x \leq 10$, $-10 \leq t \leq 10$, these effects are observed in Figures (1, 2, 3, 4), in the same interval, by selecting $t = \frac{3}{2}$, Figures (5, 6) are presented. The intervals have been maintained by $-20 \leq x \leq 20$, $-20 \leq t \leq 20$, while time has been indicated in the legend to show the influence of time development on the wave patterns for Figures (7, 8). For equations (33) and (34), the complimentary coefficients have been determined by: $v_1 = \frac{3}{4}, v_2 = -\frac{2}{3}, b = \frac{5}{2}, a_2 = -\frac{2}{3}, y = \frac{1}{4}$. While the intervals also have a great impact on the appearance of the solutions, here we choose $-10 \leq x \leq 10$, $-10 \leq t \leq 10$, these significances are reflected in Figures (9, 10, 11, 12). In the same interval, by setting $t = \frac{2}{3}$, Figures (13, 14) are introduced. The horizontal and vertical intervals have been maintained as previously, while time has been indicated in the legend to demonstrate the effect of time evolution on the wave designs for Figures (15, 16).

5 Conclusion

This work aimed to examine the exact solutions of the nonlinear fourth-order generalized Hietarinta-type problem in a (2+1)-dimensional space. This has been achieved by using the modified extended tanh − function approach. This is the first application of the approach to this model. The results of this study are novel and noteworthy concerning previous research since they present various approaches non-examined, analytically. These solutions represent in a various forms such as hybrid rational, logarithmic, hyperbolic, and trigonometric functions. Besides, two- and three-dimensional graphical representations of the solutions and two-dimensional visuals exhibiting the impacts of temporal development have been introduced. Also, two dimensional contour plots and revolving plots in three dimensions have been authenticated to better comprehend the dynamical properties of the discovered solutions. Furthermore, all obtained solutions have been confirmed by representational computational software programs by re-entering them into the main model considered. The usefulness and dependability of the technique used in analyzing the produced solutions to the aforementioned equation have been proven by the study results, which will be applied to further mathematical models. The findings reveal that the free parameters of the collected solutions strongly impact the waveform and its dynamics, possibly acting as a representation of multiple difficult and unknown features that develop across diverse scientific fields.

6 Declarations

6.1 Competing interests:

The author affirms that there is no conflict of interest related to the publishing of this work.

6.2 Funding:

Not applicable.

6.3 Author's contributions:

A.A.M.-Conception and Design, Material Preparation, Data Collection, Methodology, Analysis, Writing and Original Draft. All authors read and approved the final version of the manuscript.

6.4 Acknowledgement:

We are grateful to Editor-in-Chief Prof. Dr. Haci Mehmet Baskonus for his guidance and insights throughout this period. We appreciate the role of reviewers in providing helpful input that enhanced the quality of our paper.

6.5 Data availability statement:

The data sources collected during and/or analyzed during the present investigation are accessible from the corresponding author upon reasonable request.

6.6 Using of AI tools:

The author affirms that Artificial Intelligence (AI) techniques were not used in creating this content.

References

[1] Mahmud A.A., Tanriverdi T., Muhamad K.A., Exact traveling wave solutions for (2+ 1)-dimensional Konopelchenko-Dubrovsky equation by using the hyperbolic trigonometric functions methods, International Journal of Mathematics and Computer in Engineering, 1(1), 11–24, 2023.

[2] Muhamad K.A., Tanriverdi T., Mahmud A.A., Baskonus H.M., Interaction characteristics of the Riemann wave propa-

gation in the (2+1)-dimensional generalized breaking soliton system, International Journal of Computer Mathematics, 100(6), 1340–1355, 2023.

[3] Baskonus H.M., Mahmud A.A., Muhamad K.A., Tanriverdi T., A study on Caudrey-Dodd-Gibbon-Sawada-Kotera partial differential equation, Mathematical Methods in the Applied Sciences, 45(14), 8737–8753, 2022.

[4] Baskonus H.M., Mahmud A.A., Muhamad K.A., Tanriverdi T., Gao W., Studying on Kudryashov-Sinelshchikov dynamical equation arising in mixtures liquid and gas bubbles, Thermal Science, 26(2B), 1229–1244, 2022.

[5] Tanriverdi T., Baskonus H.M., Mahmud A.A., Muhamad K.A., Explicit solution of fractional order atmosphere-soil-land plant carbon cycle system, Ecological Complexity, 48(100966), 2021.

[6] Mahmud A.A., Tanriverdi T., Muhamad K.A., Baskonus H.M., Structure of the analytic solutions for the complex non-linear (2+1)-dimensional conformable time-fractional Schrödinger equation, Thermal Science, 27(1), 211–225, 2023.

[7] Mahmud A.A., Baskonus H.M., Tanriverdi T., Muhamad K.A., Optical solitary waves and soliton solutions of the (3+1)-dimensional generalized Kadomtsev-Petviashvili- Benjamin-Bona-Mahony equation, Computational Mathematics and Mathematical Physics, 63(6), 1085–1102, 2023.

[8] Mahmud A.A., Tanriverdi T., Muhamad K.A., Baskonus H.M., Characteristic of ion-acoustic waves described in the solutions of the (3+1)-dimensional generalized Korteweg-de Vries-Zakharov-Kuznetsov equation, Journal of Applied Mathematics and Computational Mechanics, 22(2), 36–48, 2023.

[9] Hussain A., Ali H., Zaman F., Abbas N., New closed form solutions of some nonlinear pseudo-parabolic models via a new extended direct algebraic method, International Journal of Mathematics and Computer in Engineering, 2(1), 35–58, 2024.

[10] Sivasundaram S., Kumar A., Singh R.K., On the complex properties to the first equation of the Kadomtsev-Petviashvili hierarchy, International Journal of Mathematics and Computer in Engineering, 2(1), 71–84, 2024.

[11] Mulimani M., Srinivasa K.A., Novel approach for Benjamin-Bona-Mahony equation via ultra spherical wavelets collocation method, International Journal of Mathematics and Computer in Engineering, 2(2), 39–52, 2024.

[12] Usman M., Hussain A., Zaman F., Abbas N., Symmetry analysis and invariant solutions of generalized coupled Zakharov-Kuznetsov equations using optimal system of Lie subalgebra, International Journal of Mathematics and Computer in Engineering, 2(2), 53–70, 2024.

[13] Zhao Z., He L., Space-curved resonant solitons and inelastic interaction solutions of a (2+1)-dimensional generalized KdV equation, Nonlinear Dynamics, 112, 3823–3833, 2024.

[14] Iqbal M., Lu D., Seadawy A.R., Ashraf M., Albaqawi H.S., Khan K.A., Chou D., Investigation of solitons structures for nonlinear ionic currents microtubule and Mikhaillov-Novikov-Wang dynamical equations, Optical and Quantum Electronics, 56(3), 361, 2024.

[15] Feng Y., Bilige S., Multiple rogue wave solutions of a generalised Hietarinta-type equation, Pramana, 95(3), 151, 2021.

[16] Gao D., Lü X., Peng M.S., Study on the (2+1)-dimensional extension of Hietarinta equation: soliton solutions and Bäcklund transformation, Physica Scripta, 98(9), 095225, 2023.

[17] Younas U., Sulaiman T.A., Ren J., Yusuf A., On the interaction phenomena to the nonlinear generalized Hietarinta-type equation, Journal of Ocean Engineering and Science, 9(1), 89–97, 2024.

[18] Chen S.J., Ma W.X., Lü X., Bäcklund transformation, exact solutions and interaction behaviour of the (3+1)-dimensional Hirota-Satsuma-Ito-like equation, Communications in Nonlinear Science and Numerical Simulation, 83, 105135, 2020.

[19] Younas U., Ren J., Sulaiman T.A., Bilal M., Yusuf A., On the lump solutions breather waves two-wave solutions of (2+1)-dimensional Pavlov equation and stability analysis, Modern Physics Letters B, 36(14), 2250084, 2022.

[20] Kaur L., Wazwaz A.M., Dynamical analysis of lump solutions for (3+1) dimensional generalized KP-Boussinesq equation and its dimensionally reduced e quations, Physica Scripta, 93(7), 075203, 2018.

[21] He C., Tang Y., Ma W., Ma J., Interaction phenomena between a lump and other multi-solitons for the (2+1)-dimensional BLMP and Ito equations, Nonlinear Dynamics, 95, 29–42, 2019.

[22] Alam L.M.B., Jiang X., Exact and explicit traveling wave solution to the time-fractional phi-four and (2+1) dimensional CBS equations using the modified extended tanh − function method in mathematical physics, Partial Differential Equations in Applied Mathematics, 4, 100039, 2021.

[23] Eldidamony H.A., Ahmed H.M., Zaghrout A.S., Ali Y.S., Arnous A.H., Highly dispersive optical solitons and other solutions in birefringent fibers by using improved modified extended tanh-function method, Optik, 256, 168722, 2022.

[24] Elsherbeny A.M., El-Barkouky R., Ahmed H.M., El-Hassani R.M., Arnous A.H., Optical solitons and another solutions for Radhakrishnan-Kundu-Laksmannan equation by using improved modified extended tanh-function method, Optical and Quantum Electronics, 53, 718, 2021.

[25] Rabie W.B., Khalil T.A., Badra N., Ahmed H.M., Mirzazadeh M., Hashemi M.S., Soliton solutions and other solutions to the (4+1)-dimensional Davey-Stewartson- Kadomtsev-Petviashvili equation using modified extended mapping method, Qualitative Theory of Dynamical Systems, 23(2), 87, 2024.

[26] Almatrafi M.B., Solitary wave solutions to a fractional model using the improved modified extended tanh-function method, Fractal and Fractional, 7(3), 252, 2023.

[27] Batwa S., Ma W.X., Lump solutions to a generalized Hietarinta-type equation via symbolic computation, Frontiers of Mathematics in China, 15, 435–450, 2020.
[28] Kumar S., Kumar A., A study of nonlinear extended Zakharov-Kuznetsov dynamical equation in (3+1)-dimensions: Abundant closed-form solutions and various dynamical shapes of solitons, Modern Physics Letters B, 36(25), 2250140, 2022.
[29] Kumar A., Kumar S., Dynamical behaviors with various exact solutions to a (2+1)-dimensional asymmetric Nizhnik-Novikov-Veselov equation using two efficient integral approaches, International Journal of Modern Physics B, 2450064, 2023.
[30] Kumar A., Kumar S., Dynamic nature of analytical soliton solutions of the (1+1)-dimensional Mikhailov-Novikov-Wang equation using the unified approach, International Journal of Mathematics and Computer in Engineering, 1(2), 217–228, 2023.
[31] Kumar S., Kumar A., Newly generated optical wave solutions and dynamical behaviors of the highly nonlinear coupled Davey-Stewartson Fokas system in monomode optical fibers, Optical and Quantum Electronics, 55(6), 566, 2023.
[32] Mahmud A.A., Muhamad K.A., Tanriverdi T., Baskonus H.M., An investigation of Fokas system using two new modifications for the trigonometric and hyperbolic trigonometric function methods, Optical and Quantum Electronics, 56, 717, 2024.
[33] Mahmud A.A., Application of three different methods to several nonlinear partial differential equations modeling certain scientific phenomena, (PhD Thesis), Harran University, Türkiye, 2023.
[34] Muhamad K.A., A study on some nonstandard partial differential equations, (PhD Thesis), Harran University, Türkiye, 2023.